

## Dissolution and Drug release profiles of phosphate glasses doped with high valency oxides

E. El-Meliegy<sup>1\*</sup>, M. Farag<sup>\*</sup> and J. Knowles<sup>\*\*</sup>

\* National Research Centre, Dept. of Biomaterials, El-Tahrir Street, Dokki, Cairo, Egypt.

\*\* Biomaterials and Tissue Engineering, UCL Eastman Dental Institute, University College London

### Abstract:

This paper investigates phosphate glasses incorporating Vanadium and Molybdenum oxides for effective management of dissolution and drug release. These glass formulations are found to reduce the rate of dissolution from the glass surfaces. The drug functional groups of Vancomycin molecules loaded by immersion showed stronger hydrogen bonding with Vanadium doped glasses and consequently lower rate of drug release over two weeks indicating better surface attachment with the drug molecules and slow drug release profiles. This can be explained by the strong adherence of drug molecules to glass surfaces compared with the molybdenum containing glasses (PM5 and PM10). The strong attachment relates to hydrogen bonding between the amino-functional groups of Vancomycin and the hydrated P-O-H groups in the glass network. In conclusion, the rate of dissolution of doped glasses and the rate of drug release can be administered to deliver the drug molecules over weeks.

## 1. Introduction

Because of the increase in the number of accidents, multiple trauma victims, and ageing of the population, the demand for bone reconstruction is constantly growing. Therefore, research and development of new bone grafting materials became the main interest of scientists. Calcium phosphate ceramics, such as hydroxyapatite, have been widely used as bone grafting materials, due to their similarity in chemical composition with human bone body [1]. But, too low bioresorbability rate at normal physiological conditions [2] makes a limitation to apply such materials successfully in some biomedical applications require a highly biodegradable and bioresorbable materials. However, bioactive glasses, such as phosphate-based glasses are considered desirable alternative materials. Bioactive glasses have the ability to bond with tissue [3]), as well as, the flexibility of controlling degradation by changing their chemical composition.

Calcium phosphate glasses have demonstrated a superior material for medical uses due to their sustained and controlled solubility[4], which make them potentially useful for promoting the regeneration of soft and hard tissues. Additionally, their chemical composition is close to that of the inorganic part of bone, which nominated them for use as alternative materials for silicate bioglasses. In addition, phosphate glasses are bioresorbable and biodegradable materials because of their solubility in human body [5], which allows them to be used as biodegradable suture thread and as drug delivery vehicles [6].

Recently, phosphate glasses have been used as suitable carriers for the delivery of therapeutic ions, such as silver and copper [7]. Phosphate-based glasses have previously been examined for tissue engineering applications including transition metal ions such as  $\text{Fe}^{3+}$ ,  $\text{Cu}^+$  and  $\text{Cu}^{2+}$ ,  $\text{Zn}^{2+}$ , and  $\text{Ti}^{2+}$ , which have shown to improve cell attachment, activate the synthesis of enzymes involved in the first step of protein biosynthesis and exhibit antibacterial properties [8]. Consequently, phosphate glasses are used as potential substrates in bone tissue engineering [9].

However, vanadium and molybdenum oxides are expected to modify phosphate glasses' network, and control the degradation rate of the glasses. From another view, it is proposed that their ions have a therapeutic action into the body. Vanadium compounds (such as Polyoxovanadates) have demonstrated applications in medicine and proved efficient effect

against leukemia, breast adenocarcinoma, testicular, renal, and gastrointestinal cancers and hepatomas. [10].

As well as, it was proved that vanadium has the anti-diabetic properties which was initiated in 1985 by John McNeill [11] and used as inhibitors to various phosphate-metabolizing enzymes through binding to the protein matrix. On the other hand, peroxy-molybdenum complexes have shown an antitumor effect [12]. However, despite the proven therapeutic values of vanadium and molybdenum compounds in biomedicine, there is no clear evidence about the suitability of phosphate glasses as drug delivery carriers.

Thus, the application of phosphate glasses in drug delivery systems could be very useful, but their fast degradation behavior is hindering the application in this approach. Therefore, number of high valency elements was suggested as dopants into phosphate glasses in order to control the rate of dissolution and in role, improve the degradation profile of glasses for a therapeutic action. The phosphate glasses modified with the Vanadium and Molybdenum will be evaluated for local drug delivery carriers. This fact would be successful, if it could be possible to modify the controlled dissolution and potential biodegradation.

In this work, vanadium and molybdenum doped phosphate glasses will be prepared in a trial to control the degradation rates and ion release of phosphate glasses and investigate their use as drug delivery carriers. Vancomycin antibacterial drug was selected as a drug model in this study due to its broad-spectrum antibiotic ability to treat serious infections, which may be associated with application of bone-filling materials, orthopedic implants or bone replacements.

## **2. Materials and methods**

### **2.1. Glass preparation**

The base phosphate glasses were prepared by melting. The chemical compositions of the studied phosphate glasses in Mol% are shown in Table 1. The glass compositions formulated using  $\text{NaH}_2\text{PO}_4$  99.0% Sigma, calcium carbonate ( $\text{CaCO}_3$ ) 99% Sigma aldrich, Phosphorus pentoxide ( $\text{P}_2\text{O}_5$ ) 99% Sigma Aldrich and Vanadium(V) oxide ( $\text{V}_2\text{O}_5$ ) 99.6% Aldrich and Molybdenum(IV) oxide ( $\text{MoO}_2$ ) 99% Aldrich. The precursors were weighed to satisfy the proposed glass formulations and placed into a 200ml platinum crucible. Care was taken while weighing Phosphorus pentoxide in order to avoid moisture content. The crucible is

placed into a furnace at temperature 750- 1200°C for 1h according to the melting point of the glass batches.

The molten glasses were then poured into a preheated graphite molds in order to design glass blocks by casting. The glass blocks were annealed at the right annealing temperature according to the results of thermal analysis, at 350 °C/1h, and then allowed to cool to room temperature, in order to remove the residual stresses in the glass. The glass rods were obtained and cut into 12 mm diameter, 2 mm thick discs using a diamond saw.

## **2.2. Characterization of glasses**

### **2.2.1. DTA**

Glass powders were prepared grinding and screened to pass a 75µm sieve. The thermal characterization was carried out using a Setaram differential thermal analyzer (Setaram, France). Powder glass samples were scanned at a heating rate of 10°C/min up to 1000°C in order to determine glass transition ( $T_g$ ), crystallization ( $T_c$ ), and ( $T_m$ ) melting temperatures.

### **2.2.2. Fourier Transform Infrared Spectroscopy**

The infrared absorption spectra of the phosphate glass powders were analyzed at room temperature in the wave number range of 4000–400 $\text{cm}^{-1}$  using Fourier transform infrared (JASCO FT/IR-4600). The 2mg samples were mixed with 200mg KBr in an agate mortar and pressed into a pellet. For each sample, the FTIR spectrum was normalized with a blank KBr pellet.

### **2.2.3. In vitro degradation test**

In vitro degradation test was performed by determining the concentrations of ions released from the glasses upon immersion of bulk glass discs (13mm diameter and 2mm thick) in tris-HCl buffer solution.[13]. The concentrations of ions (calcium, phosphorus, molybdenum and vanadium ions) released into the solution and pH of incubated solutions were measured at the predetermined times (1, 3, 7, 18 and 28days). On the other hand, the effect of solution on the glass surfaces was examined by SEM-EDX (Model Quanta 250 FEG) after immersion in SBF (simulated body fluid) for 1 week. SBF was prepared according to Kokubo 2006 [14].

### **2.2.4. Drug delivery experiment**

#### **Drug Loading:**

The glass powder samples (200 mg) were loaded with vancomycin-HCl through immersion in 10 ml drug solution (5 mg/ml) for 2 days under static condition. The drug solutions were

collected, and the absorbance was measured by UV-visible spectroscopy at wavelength 282nm. The concentrations of non-adsorbed drug were determined by plotting the absorbance on the standard curve.

#### **Drug release:**

For drug release evaluation, each sample was immersed in 10 ml of tris-HCl buffer solution, pH 7.4, at 37 °C up to 30 days. At each predetermined time (1, 3, 6, 12 hours, 1, 3, 7, 14, 21 and 30 days), 2 ml of immersed solution was collected and replaced by 2 ml fresh tris-HCl buffer solution. The collected solutions were kept at -20°C up till the measurement. The concentrations of released drug in the collected solutions were determined by measuring the absorbance using UV-visible spectrophotometer at wavelength 282nm (Unico UV2000, n=3). The concentrations were calculated by comparison with the standard curve.

### **3. Results and discussion:**

#### **3.1. Thermal analysis**

The DTA patterns shown in Table 2 and Figure 1a displayed peak midpoint of the glass transition temperature, the crystallization and melting temperatures of the different glasses under investigation. The glass transition temperatures ( $T_g$ ), were found to increase by the increase in the  $MoO_3$  and  $V_2O_5$  contents. The transition temperature ( $T_g$ ) are 405°C, 407, 435, 447, and 477°C for P0, PM5, PM10, PV5 and PV10, respectively. The obvious increase of the transition temperatures could be attributed to the higher ionic field strength (IFS) of  $Mo^{6+}$  (2.15) and  $V^{5+}$  cations compared with that of  $Na^+$  (0.19) according to Dietzel [15]. Therefore,  $Mo^{6+}$  and  $V^{5+}$  bonds are stronger than  $Na^+$  bonds. Thus, more energy would be required to break these bonds.

Moreover, all glass samples showed two crystallization peaks and two melting temperatures peaks indicating the possibility of evolving two crystalline phases on further higher temperature heat treatment. The second exothermic peaks of crystallization ( $T_{c2}$ ) of glasses containing Mo were stronger and sharper, but at lower temperature compared with those obtained by V- containing glasses as shown in Table 2.

Alternatively, both  $T_{m1}$  and  $T_{m2}$  melting temperatures of the vanadium containing group were lower than the corresponding melting temperatures of molybdenum containing group. Where,  $T_{m1}$  temperatures were 734, 766 °C for PM5 and PM10, and 720, 670°C for PV5 and

PV10, respectively, while  $T_{m2}$  temperatures were 799, 824 °C for PM5 and PM10, and 766, 796 °C for PV5 and PV10, respectively, as shown in Fig. 1 and Table 2.

### 3.2. FTIR

The results of FTIR spectra of P0, PM5, PM10, PV5 and PV10 glasses in the frequency region between 4000 and 400  $\text{cm}^{-1}$  are shown in Figure 2. A broad band is located around 3463  $\text{cm}^{-1}$ . This band could be attributed to symmetric stretching of O–H groups in  $\text{H}_2\text{O}$  molecules that might be originated from absorbed water. The band becomes sharper and stronger with increasing the content of  $\text{MoO}_3$  or  $\text{V}_2\text{O}_5$ . Furthermore, the band located around 1636  $\text{cm}^{-1}$  is assigned to bending vibration mode of P-O-H. [16]. The results reflect the increase in covalent character of the P–O bonds with the increase of the  $\text{MoO}_3$  or  $\text{V}_2\text{O}_5$  contents and the increase of O-H bond length [17].

Moreover, the band appeared near to 490  $\text{cm}^{-1}$ , is attributed to O-P-O bending vibration mode [18]. The band near to 509  $\text{cm}^{-1}$  was assigned to harmonic of the P=O bending vibration [19]. The bands observed around 903  $\text{cm}^{-1}$  and 745  $\text{cm}^{-1}$  are attributed to asymmetric stretching and symmetric stretching modes of the bridging oxygen atoms bonded to a phosphorus atom (P–O–P) in a  $Q^2$  phosphate tetrahedron [20]. Both bands were shifted to higher frequencies with the content of the  $\text{MoO}_3$  or  $\text{V}_2\text{O}_5$ . The bands allocated around 970  $\text{cm}^{-1}$  and 1093  $\text{cm}^{-1}$  were attributed to symmetric stretching of non-bridging oxygen (NBOs) in  $Q^0$  tetrahedra [21], and asymmetric stretching vibration of P-O-P of the group ( $\text{PO}_3^{-2}$ ) [22]. The band observed at 1122  $\text{cm}^{-1}$  is assigned to the symmetric stretching vibrations of  $\text{PO}_3^{-2}$  groups [23]. The band noted at 1161  $\text{cm}^{-1}$  attributed to the symmetric stretching vibration mode of O-P-O [24]. The band presented near to 1244  $\text{cm}^{-1}$  is assigned to P=O asymmetric stretching vibration of  $\text{PO}_2$  [25], such band was increased with increase of Mo and V cations.

From FTIR results it could be noted that, the intensities of different vibration bands of phosphate structures increased by increase in the content of  $\text{MoO}_3$  or  $\text{V}_2\text{O}_5$ . Such oxides increased the number of non-bridging oxygens (NBOs) in the phosphate network, but in parallel, they acted as ionic cross-linker among NBOs, and thus, increase the ionic bond strength and decrease the P-O bonds.

### 3.3. Glass solubility

#### 3.3.1. Weight loss

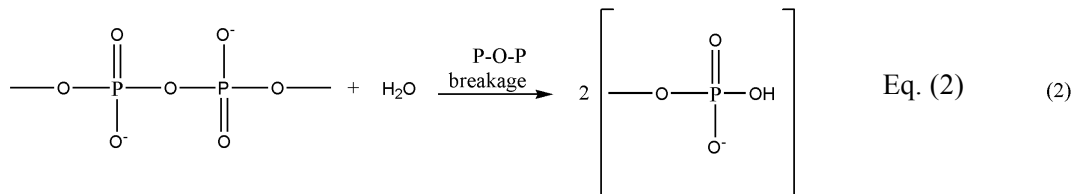
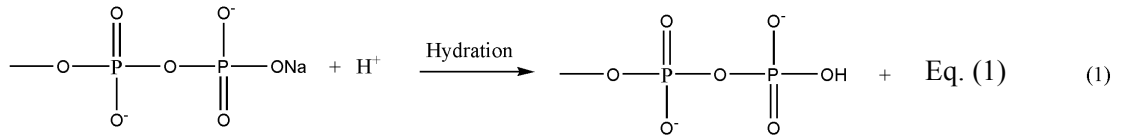
The weight loss percentage vs. the time is represented in Figure 3. It could be elucidated that the solubility of glass decreased with the addition of  $\text{MoO}_3$  and  $\text{V}_2\text{O}_5$ . Moreover, the solubilities of vanadium-containing glasses are lower compared with that of molybdenum-containing glasses. The weight loss percentages of the phosphate glasses (P0, PM5, PM10, PV5 and PV10) are found 26.9%, 9.9%, 5.5%, 2.2% and 1.7%, respectively at the end of incubation period (28 days). The fact that agree with conclusion previously reported that the addition of transition metal oxides reduce significantly the degradation of glass [26].

The addition of  $\text{MoO}_3$  or  $\text{V}_2\text{O}_5$  oxides increased the bonding strength of glass network as a result of the increase in the ionic field strength compared with  $\text{Na}_2\text{O}$ . In the current work a progressive increase in the concentrations of released  $\text{Mo}^{6+}$  and  $\text{V}^{5+}$  cations results in a substantial increase in the ionic strength of the incubation medium. Therefore, the incorporation of  $\text{MoO}_3$  and  $\text{V}_2\text{O}_5$  in the phosphate glasses decreased the dissolution rates of as a result of the spontaneous increase in the electrostatic interactions in the hydrated layer [27].

### 3.3.2. pH measurements

The pH of incubated medium of the studied phosphate glasses as a function of time are shown in Figure 4. The pH values decreased continuously in all cases to the minimum values after 7 days of incubation. The pH values were found 5.79, 6.09, 6.03, 6.10 and 6.49 for P0, PM5, PM10, PV5 and PV10, respectively. Thereafter, for incubation time more than 1 week, pH values were found continuously increasing to reach 7.00, 7.40, 7.41, 8.06 and 8.53, for P0, PM5, PM10, PV5 and PV10 glasses, respectively. The incubated medium of the base glass showed the lowest pH values as a result of generating acidic species by the dissolution of phosphorus cations released from the breakage of P–O–P bonds associated with the  $[\text{PO}_4]$  units.

According to the previously stated theory of glass dissolution [28], the phosphate glasses under investigation dissolve in aqueous medium in two steps; the hydration step and the breakage step. The hydration step, where a hydrated layer is formed on the glass surface as a result of  $\text{Na}^+$  and  $\text{H}^+$  exchange, as represented in Equation(1). The breakage step, where, the continuous attack of water results in breaking up of P-O-P bonds and accordingly breaking of glass network and release of  $[\text{PO}_4]$  units, as represented in Equation (2).



Accordingly, the incorporation of MoO<sub>3</sub> and V<sub>2</sub>O<sub>5</sub> oxides on the extent of Na<sub>2</sub>O results in reducing the rate of hydration and the rate of breakdown of the phosphate bonds. Accordingly, the rate of dissolution is found to decrease and the value pH is shown increase. However, a linear increase of pH values might be attributed to the release of Ca<sup>2+</sup> ions into the solution and chelation with the released phosphate species. Furthermore, Na<sup>+</sup> ions released into the solution due to the H<sup>+</sup> ion-exchange might take part in an increase of pH. Expectedly, the amount of phosphate species chelating with released Mo<sup>6+</sup> and V<sup>5+</sup> ions was larger, because of their high valency states.

### 3.3.3. Ions release concentrations

The ionic release of Ca<sup>2+</sup>, P species, Mo<sup>6+</sup> and V<sup>5+</sup> are shown in Figures 5-7. The dissolution curves of Ca<sup>2+</sup>, P ions (Figure 5-6) showed non-linear release. Accordingly, P0 glass represented the highest calcium ion release followed by PM5 sample. While, it showed a nearly steady state release associated with PM10 and PV10 glasses. Thus, the incorporation of Mo and V oxides into the glass networks decreased the degradation of glass, and hence, decreased the leaching of ions from glass network. On the other hand, for P0, PM10 and PV10, the maximum P- ion concentration recorded after 7 days, while, it was nearly constant release for PM5 and PV5. However, these results might be apparently different from pH values mentioned because of the complex and repeated dissolution-deposition of phosphorus in the solution. As it was expected, the concentrations of released ions; Mo and V, increased linearly with the progress of time, Figure 7.



### **3.3.4. Effect of SBF on surfaces of the studied phosphate glasses:**

SEM micrographs coupled with EDX analysis of P0, PM5, PM10, PV5 and PV10 after immersion in SBF for 1 week are shown in Figure 8. The micrographs represented that some spherical aggregates were detected on P0 glass surface, which it might be some kind of precipitated Ca-phosphate species. While, the surface of PM5 glass was smooth, looked like adjacent air bubbles and there was no connected longitudinal grooves like that observed on the surface of PM10 glass. Furthermore, there were no hydroxyl carbonate apatite detected on the surfaces of PM5 and PM10 glass. In contrary, flower-shaped crystals are found on the surfaces of PV5 and PV10 glasses, such crystals more likely formed by the deposition of released vanadium and phosphate ions. These results are confirmed by EDX elemental analyses (wt%) of glasses surfaces, as shown in Table 3.

The percentages of vanadium element on the surfaces of PV5 and PV10 glasses were much more than the corresponding percentages of molybdenum element detected on PM5 and PM10 glasses surfaces. The results of Mo and V ions concentrations in the incubating liquid (as mentioned before) were opposite. This proved that surfaces of V-containing glasses covered by crystal layer mainly composed of vanadium, and the released vanadium ions consumed to form such crystals.

### **3.4. Drug release profile**

The in vitro Vancomycin release of the different phosphate glasses (P0, PM5, PM10, PV5 and PV10) over a period of 14 days are shown in Figure 9. All glasses have the same drug release profile, whereas, the release was mainly divided into two stages. The first stage is a burst release occurring during the first day of incubation, and the second stage is observed along the rest time of immersion showing a sustained drug release. The base phosphate glass (P0) showed the highest rate of release whereas more than 90% of the drug is released at the end of the incubation period.

Alternatively, the incorporation of the high valence oxides affected obviously the rate of drug release. The phosphate glasses doped with Mo and V oxides showed lower rates of drug release. The release percentages of drug molecules of the glasses were found about 25%, 25%, 45%, 55% and 70% in PV5, PV10, PM5, PM10 and P0 respectively, in the first day of incubation. The release percentages of PM5, PM10, PV5 and PV10 were found about 72.5%, 86.8%, 54.5% and 44.8%, respectively, at the end of incubation time. Interestingly,

Vanadium containing glasses (PV5 and PV10) demonstrated lower rate of drug release. This means that the drug is strongly adhered to their surfaces compared with the Mo-containing glasses (PM5 and PM10). The results might be explained by the concept of hydrogen bonding between the hydroxyl and amino-functional groups in the Vancomycin and the hydrated P-O-H groups in the phosphate glass network [29].

A representation for the way of attachment of vancomycin molecules to the surfaces of molybdenum and vanadium doped phosphate glasses are shown in Figure 10. The diagram is based on the hydrogen bonding of drug molecules to the glass surfaces. The ionic field strength of vanadium is stronger than that of molybdenum, thus, a larger dipole effect and therefore a larger effective negative charge on the oxygen for hydrogen bonding. When the V-O bond became in contact with the drug, it formed stronger hydrogen bonding between the oxygen and the drug functional groups. Vanadium doped glasses displayed better surface attachment with the drug molecules showing a sustained drug release profile over the two weeks following the first day of incubation.

To determine the in vitro release mechanism of Vancomycin drug from different glasses, different dissolution data were fitted to two known release models; Higuchi[30] and Korsmeyer-Peppas [31]. The kinetic equations, and the regression coefficient,  $R^2$ , were used as an indication of data fitting. The different kinetic equations are;

Higuchi model [30] which is useful for studying the release of water soluble and poorly soluble drugs from variety of matrices, including solids and semi solids is being represented by equation (1):

$$Q_t = K_H t^{1/2} \quad (1)$$

Korsmeyer-Peppas model [31] is being represented by equation (2):

$$Q_t / Q_0 = K_K t^n \quad (2)$$

To find out the mechanism of drug release, first 60% drug release data were fitted in such model. Where  $Q_t$  is the amount of drug released in time  $t$ ,  $Q_0$  is the initial amount of drug in the sample,  $K_H$  and  $K_K$  are Higuchi and Korsmeyer-Peppas constants, and  $n$  is kinetic exponent. In order to determine which model is suitable for drug release kinetics, the regression coefficients,  $R^2$ , were calculated by regression analysis. Peppas [32] used this  $n$  value in order to characterize the drug release mechanism. The values of  $n$  and their corresponding release mechanism are represented in Table 4. For the case of cylindrical

tablets,  $0.45 = n$  corresponds to a Fickian diffusion mechanism,  $0.45 < n < 0.89$  attributed to non-Fickian transport,  $n = 0.89$  to Case II (relaxational) transport, and  $n > 0.89$  to super case II transport. The kinetic exponent,  $n$ , can be determined by plotting of log cumulative percentage drug release versus log time.

The regression coefficient,  $R^2$ , and release rate (KH) calculated from Higuchi model, and Regression coefficient,  $R^2$ , and kinetic exponent,  $n$ , calculated from Korsmeyer-Peppas are shown in Figure 9 and Table 5. It was noted from  $R^2$  comparison that the in vitro release profiles of Vancomycin from all glass samples could be best expressed by Korsmeyer-Peppas ( $R^2 > 0.9$ ), and the  $n$  values of this model for PM5, PM10, PV5 and PV10 samples were lower than 0.45. The drug release mechanism for all glass formulations followed Fickian diffusion (i.e. controlled release). On the other hand, the values of  $n > 0.45$  for P0 glass indicating that the dissolution of the base glass follows non-Fickian diffusion. Accordingly, two simultaneous processes happened; drug diffusion and glass erosion. Alternatively, the release profiles of PV5 and PV10 samples could be expressed by Higuchi model, which indicated that diffusion was the predominant mechanism of drug release from such samples. Interestingly, it could be tailored the release mechanism by changing the glass composition.

#### **Conclusion:**

The dissolution and drug release profiles of phosphate glasses incorporating vanadium and Molybdenum oxides were investigated. The rate of glass dissolution is found to be reduced through the slow leaching of ions from the glass surfaces with the presence of high valance oxides.

Vanadium doped glasses (PV5 and PV10) demonstrated lower rate of drug release in the period following the first day of drug release indicating a slow drug release profiles compared with the molybdenum containing glasses (PM5 and PM10).

The slow drug release rate relates to the hydrogen bonding between the hydroxyl and amino-functional groups in the Vancomycin and hydrated P-O-H groups in the phosphate glass network.

In conclusion, the rate of dissolution of doped glasses and the rate of drug release can be administered to deliver the drug molecules over several weeks.

## References

1. El-Meliigy E. and Noort R. V., Glasses and Glass Ceramics for Medical Applications, Springer New York, London, ISBN: 978-1-4614-1227-4, December (2012)
2. Baksh D, Davies JE. Design strategies for 3-dimensional in vitro bone growth in tissue-engineering scaffolds. In: Davies JE, editor. Bone engineering, Toronto, Canada, 2000. p. 488–95.
3. Ahmed I, Lewis M, Olsen I and Knowles JC, Phosphate glasses for tissue engineering: Part 2. Processing and characterisation of a ternary-based P<sub>2</sub>O<sub>5</sub>-CaO-Na<sub>2</sub>O glass fibre system, *Biomaterials*. 2004 Feb; 25(3):501-7.
4. Navarro M, Clement J, Ginebra MP, Martinez S, Avila G, Planell JA. Improvement of the stability and mechanical properties of resorbable phosphate glasses by the addition of TiO<sub>2</sub>. Proceedings of the 14th International Symposium on Ceramics in Medicine, *Bioceramics* 14, Palms Springs, USA 2002. p. 275–8.
5. Y. Zhang, M.A. Lopes, J.D. Santos, *Bioceram. Key Eng. Mater.* 192 (2000) 643.] [M. Uo, M. Mizuno, Y. Kuboki, A. Makishima, F. Watari, *Biomaterials* 19 (1998) 2277
6. C.F. Drake, W.M. Allen, *Biochem Soc Trans* 13 (1985) 516.] [S.N. Bhaskar, J.M. Brady, L. Getter, M.F. Grower, T. Driskell, *Oral Surg.* 32 (1971) 336.] [J. Burnie, T. Gilchrist, S.R.I. Duff, C.F. Drake, N.G.L. Harding, A.J. Malcom, *Biomaterials* 2 (1981) 244.
7. U. Ploska, G. Berger, *Biomaterials* 18, 24, 1671 (1997).] [ J. C. Knowles, K. Franks, I. Abrahams, *Biomaterials* 22, 23, 3091 (2001).] [M. T. Fulmer, I. C. Ison, C. R. Hankermayer, B. R. Constantz, J. Ross, *Biomaterials* 23, 3, 751 (2002)
8. Pickup DM, Newport RJ, Knowles JC, Sol-gel phosphate-based glass for drug delivery applications, *J Biomater Appl.* 2012 Jan;26(5):613-22
9. Sanzana ES<sup>1</sup>, Navarro M, Macule F, Suso S, Planell JA, Ginebra MP, Of the in vivo behaviour of calcium phosphate cements and glasses as bone substitutes, Acta Biomater. 2008 Nov;4(6):1924-33
10. E. Kioseoglou, A. Salifoglou, *J. Agroaliment. Process. Technol.*, 17 (2011), pp. 239–241
11. C.E. Heyliger, A.G. Tahiliani, J.H. Mcneill *Science*, 227 (1985), p. 1474
12. A. Maniatakou, S. Karaliota, M. Mavri, C.P. Raptopoulou, A. Terzis, A. Karaliota, J. *Inorg. Biochem.*, 103 (2009), pp. 859–868] [M. Grzyna, W. Lasocha, *J. Mol. Struct.*,

- 888 (2008), pp. 318–326] [M. Grzywa, W. Nitek, W. Lasocha, Elsevier Sc. B.V., Amsterdam, 2009
13. Kokubo T., Takadama H., How useful is SBF in predicting in vivo bone bioactivity. *Biomaterials*, 2006, 27: 2907–2915.
  14. Kokubo T., Takadama H., How useful is SBF in predicting in vivo bone bioactivity. *Biomaterials*, 2006, 27: 2907–2915.
  15. Dietzel AZ. Die Kationenfeldstärken und ihre Beziehungen zu Entglasungsvorgängen, zur Verbindungsbildung und zu den Schmelzpunkten von Silicaten. *Z Elektrochem* 1942;48:9–23.
  16. P. Y. Zavalij and M. S. Whittingham, *Acta Cryst.*, 1999, B55, 627
  17. S.M. Abo-Naf, N.A. Ghoneim, H.A. El-Batal, *J. Mater. Sci.: Mater. Electron.* 15 (2004) 273.] [Md. Rafiqul Ahsan, M. Golam Mortuza, *J. Non-Cryst. Solids* 351 (2005) 2333.
  18. F.H. ElBatal, M.A. Marzouk, A.M. Abdelghany, UV–visible and infrared absorption spectra of gamma irradiated V2O5-doped in sodium phosphate, lead phosphate, zinc phosphate glasses: A comparative study *Journal of Non-Crystalline Solids* 357 (2011) 1027–1036
  19. A.A. Kader, A.A. Higazy, M.M. Elkholy, *J. Mater. Sci.: Matter. Electron.* 2 (3) (1991) 157–163.
  20. A.A. Kader, A.A. Higazy, M.M. Elkholy, *J. Mater. Sci.: Matter. Electron.* 2 (3) (1991) 157–163.
  21. Carta D, Pickup DM, Knowles JC, Ahmed I, Smith ME, Newport RJ. A structural study of sol-gel and melt-quenched phosphate-based glasses. *J Non-Cryst Solids* 2007;353:1759.] [Shih PY. Properties and FTIR spectra of lead phosphate glasses for nuclear waste immobilization. *Mater Chem Phys* 2003;80:299.
  22. L. Pavic, A.M. Milankovic, P.R. Rao, A. Santic, V.R. Kumar, N. Veeraiah, *J. Alloy Compd.* 604 (2014) 352–362.
  23. Abou Neel EA, Chrzanowski W, Valappil SP, O’Dell LA, Pickup DM, Smith ME, et al. Doping of a high calcium oxide metaphosphate glass with titanium dioxide. *J Non-Cryst Solids* 2009;355:991.
  24. A. Shaim, M. Et-tabirou, *Mat. Chem. Phys.* 80 (2003) 63–67.

25. L.G. Saout, P. Simon, F. Fayon, A. Blin, Y. Vaills, J. Raman Spectrosc. 33 (2002) 740–746.
26. Karabulut M, Metwalli E, Day DE, Brow RK. Mossbauer and IR investigations of iron ultraphosphate glasses. J Non-Cryst Solids 2003;328:199.
27. Delahaye F, Montagne L, Palavit G, Touray JC, Baillif P. Acid dissolution of sodium–calcium metaphosphate glasses. J Non- Cryst Solids 1998;242:25–32.
28. E. Fernandez, F.J. Gil, M.P. Ginebra, et al., Calcium phosphate bone cements for clinical applications: Part 1. Solution chemistry, Journal of Materials Science. Materials in Medicine 10 (1999) 169 – 176.] [L.L. Hench, Physical chemistry of glass surfaces, Journal of Non-Crystalline Solids 25 (1977) 343 – 369.] [[18] J.O. Isard, A.R. Allnatt, P.J. Melling, et al., An improved model of glass dissolution, Physics and Chemistry of Glasses 23 (6) (1982) 185 – 189.
29. M. Zhu, J. Zhang, C. Tao, X. He, Y. Zhu, Design of mesoporous bioactive glass/hydroxyapatite composites for controllable co-delivery of chemotherapeutic drugs and proteins Mater. Lett., 2014, 115, 194-197
30. Higuchi T. Mechanism of sustained action medication. Theoretical analysis of rate of release of solid drugs dispersed in solid matrices. J Pharm Sci. 1963; 52:1145-1149.
31. Korsmeyer, R.W., Gurney, R., Doelker, E., Buri, P., Peppas, N.A., Mechanisms of solute release from porous hydrophilic polymers. Int. J. Pharm., 15 (1983) 25-35.
32. Peppas, N.A., 1985. Analysis of Fickian and non-Fickian drug release from polymers. Pharm. Acta Helv. 60, 110–111.

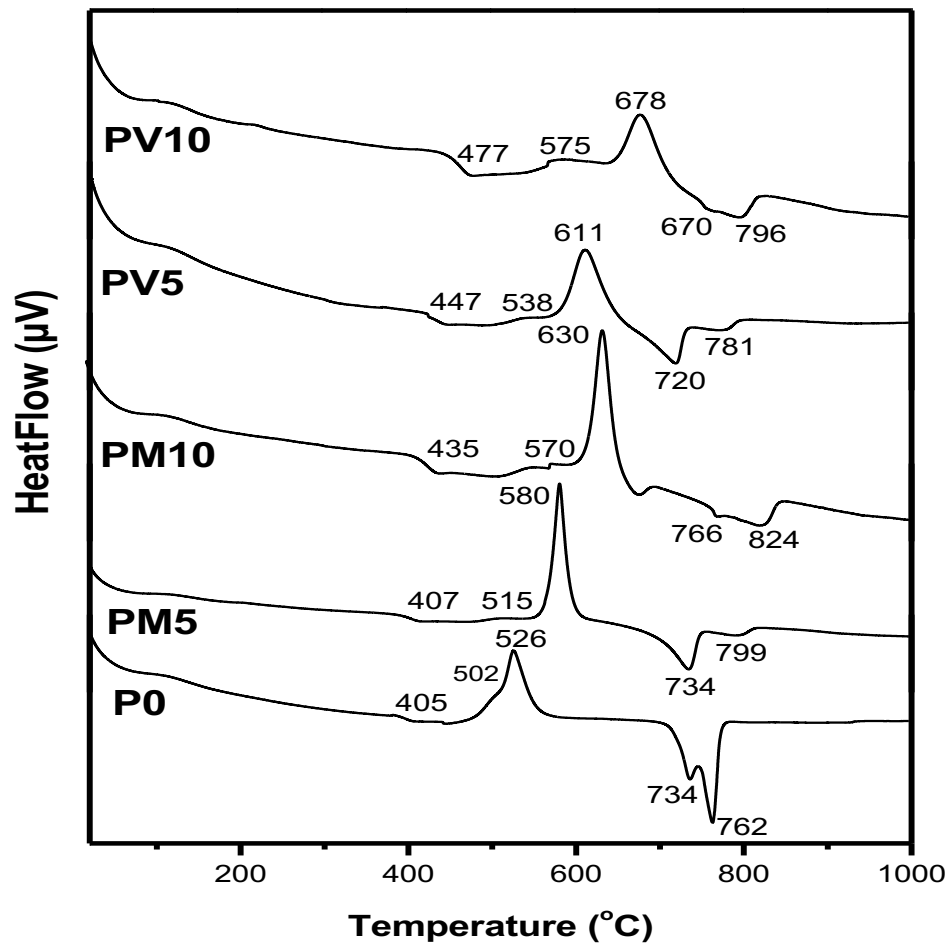


Figure 1. DTA patterns of the different phosphate glasses

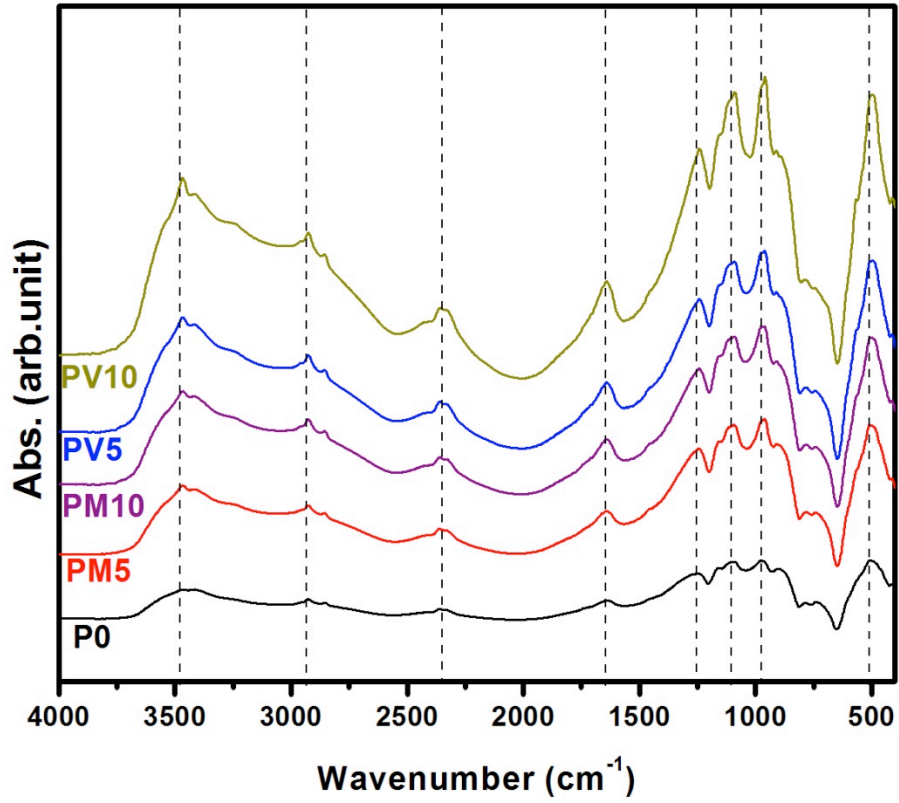


Figure 2. FT-IR spectra of the different phosphate glasses

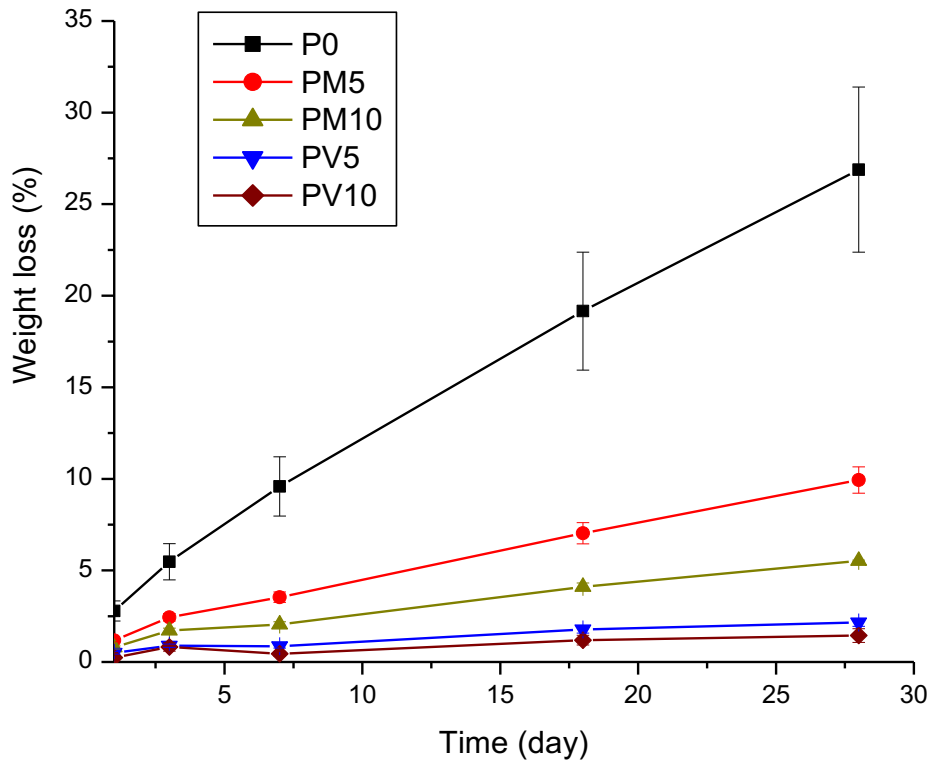


Figure 3. weight loss % of P0, PM5, PM10, PV5 and PV10 glass samples as a function of time.



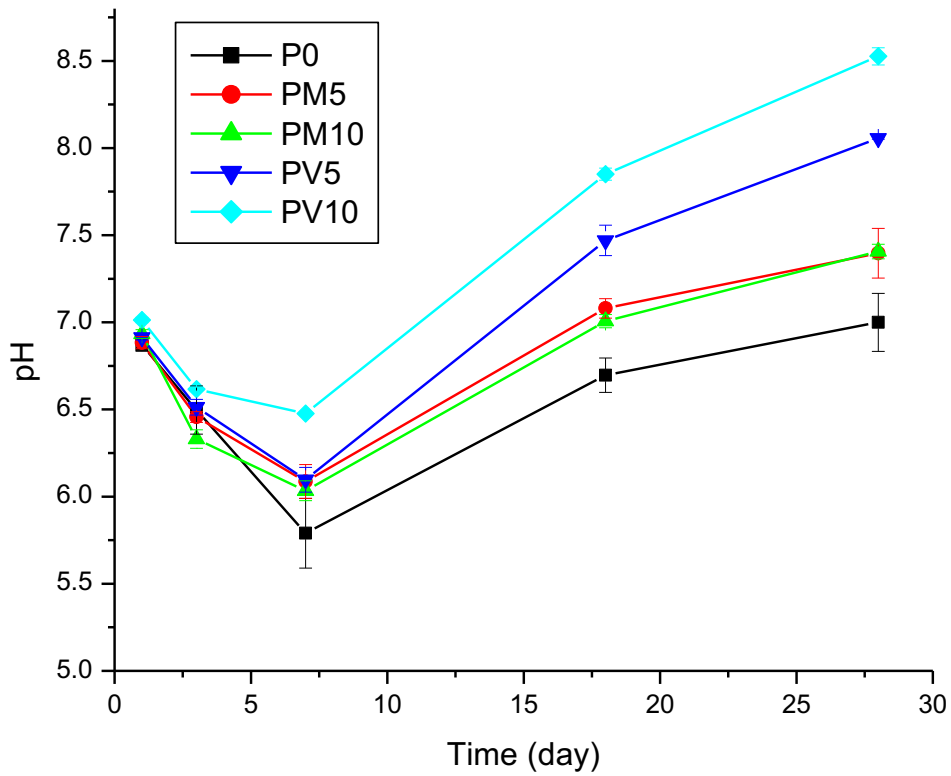


Figure 4. pH of P0, PM5, PM10, PV5 and PV10 glass samples as a function of time.

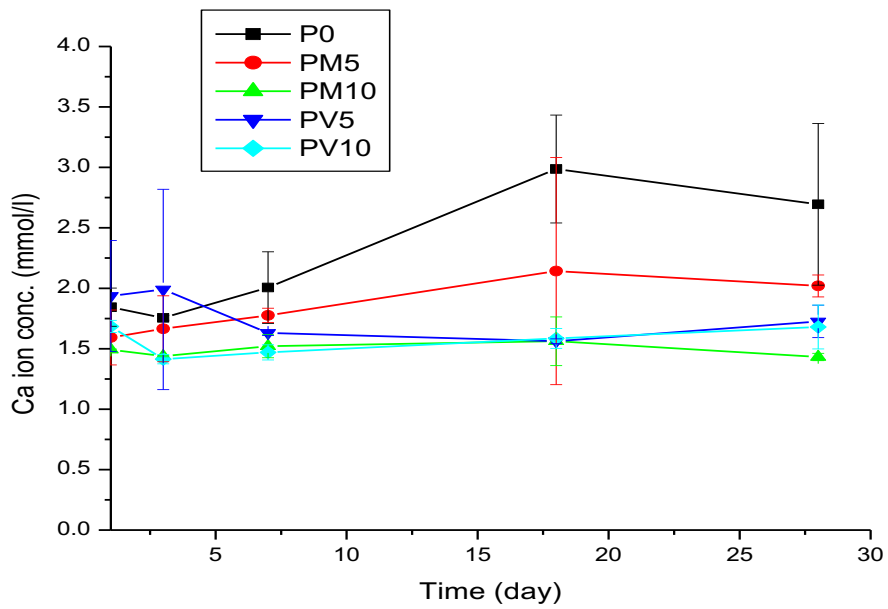


Figure 5. Release of Calcium cations from the phosphate glasses (P0, PM5, PM10, PV5 and PV10) as a function of time

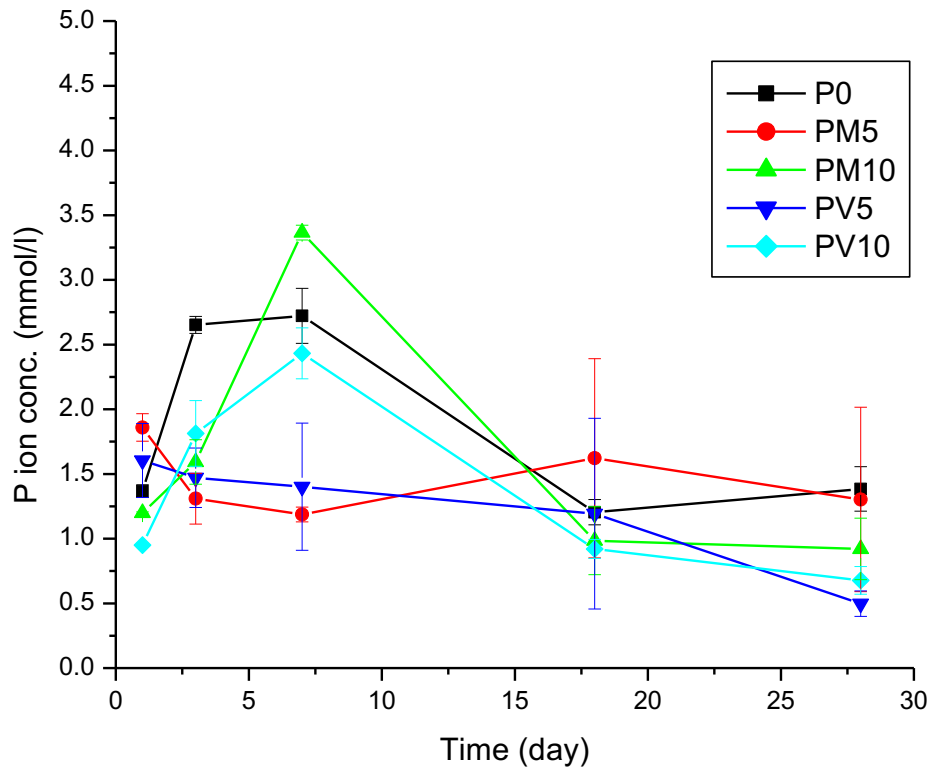


Figure 6. Release of phosphorous cations from the phosphate glasses (P0, PM5, PM10, PV5 and PV10) as a function of time

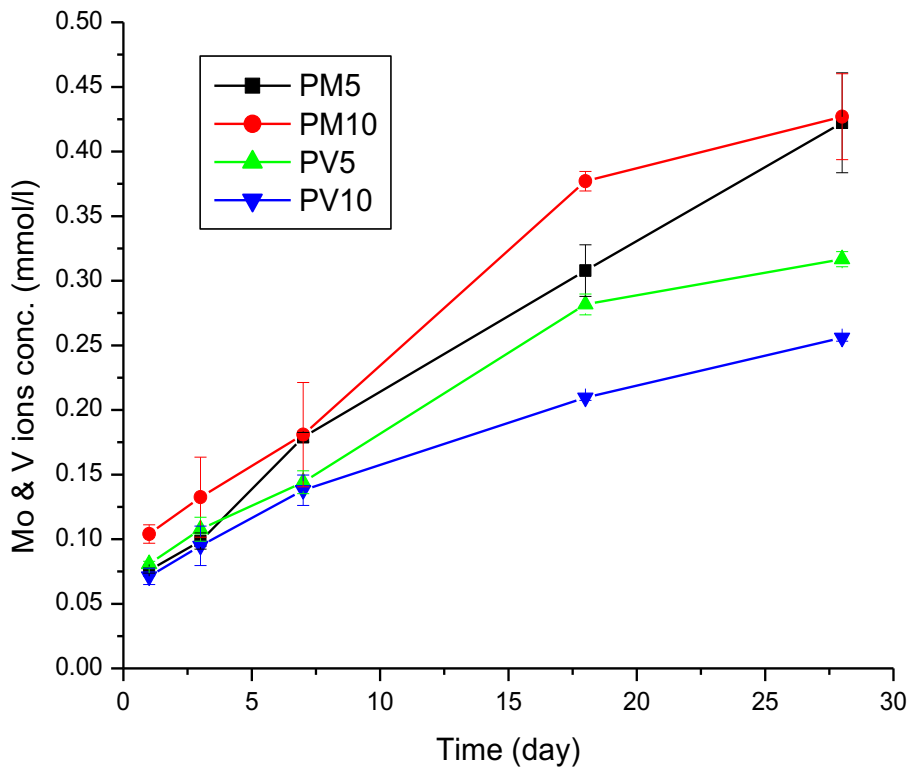


Figure 7. Release of molybdenum and vanadium cations from the phosphate glasses (P0, PM5, PM10, PV5 and PV10) as a function of time

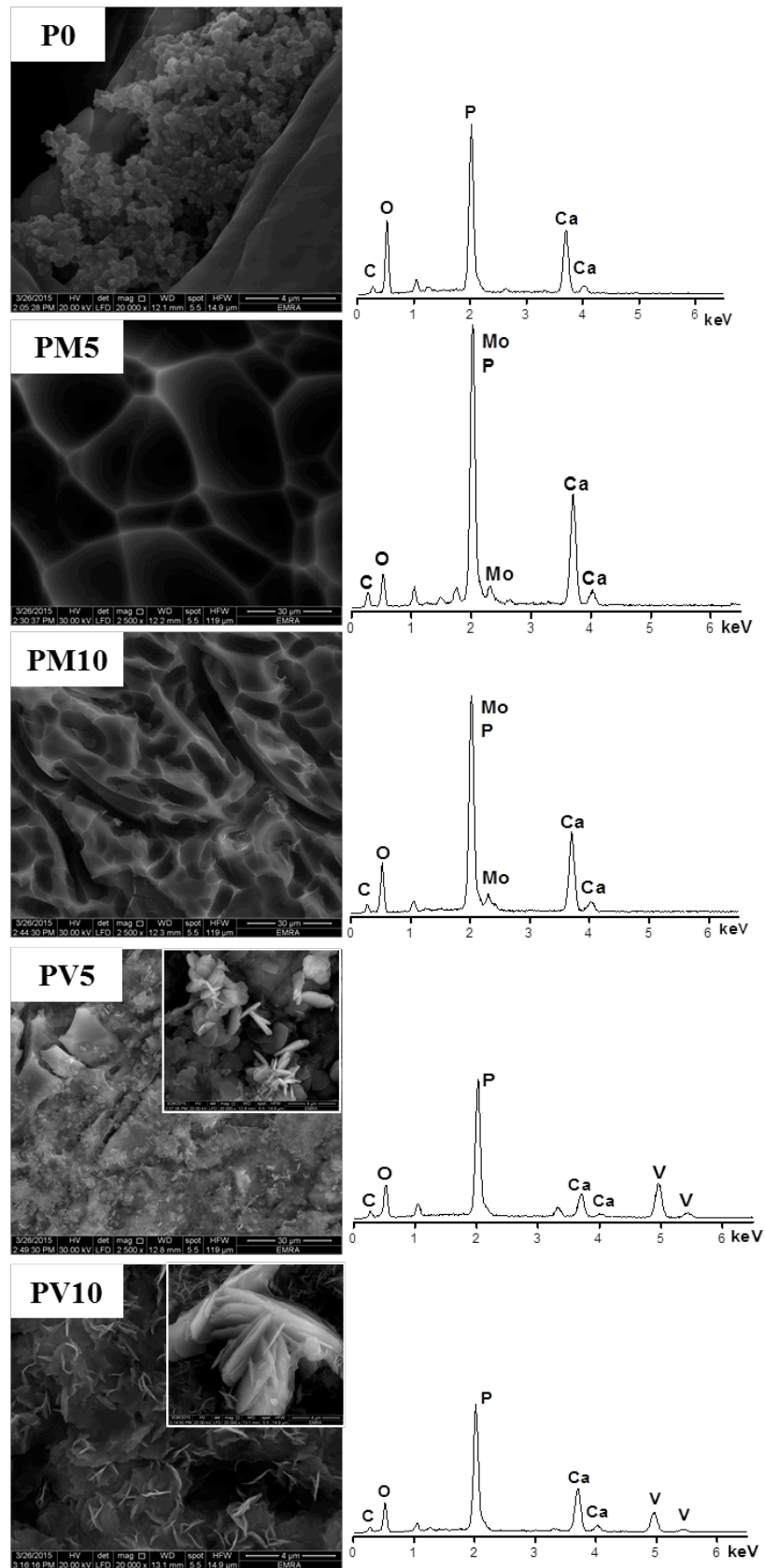
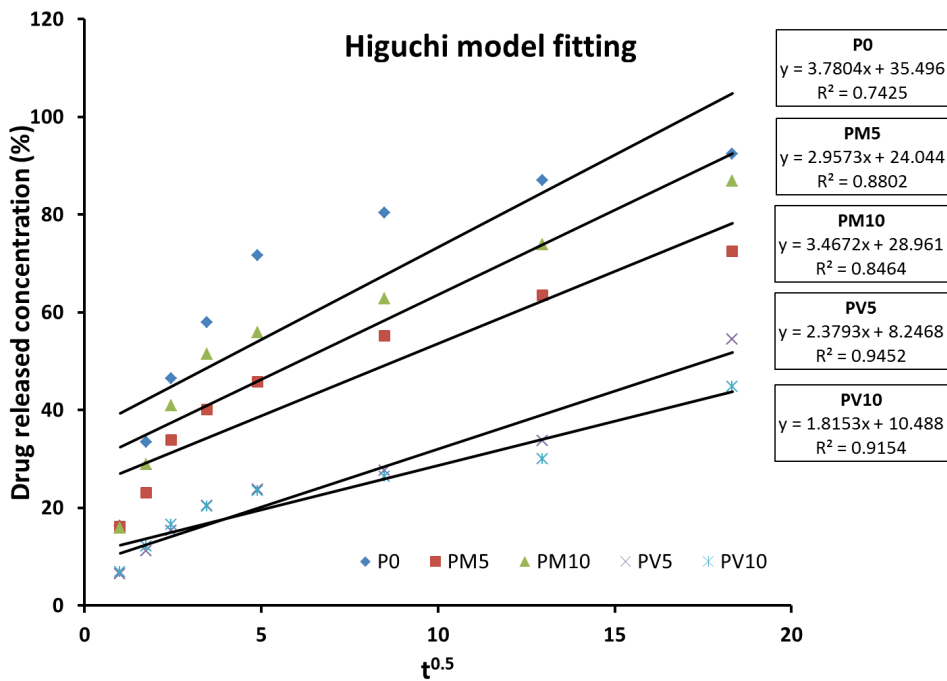
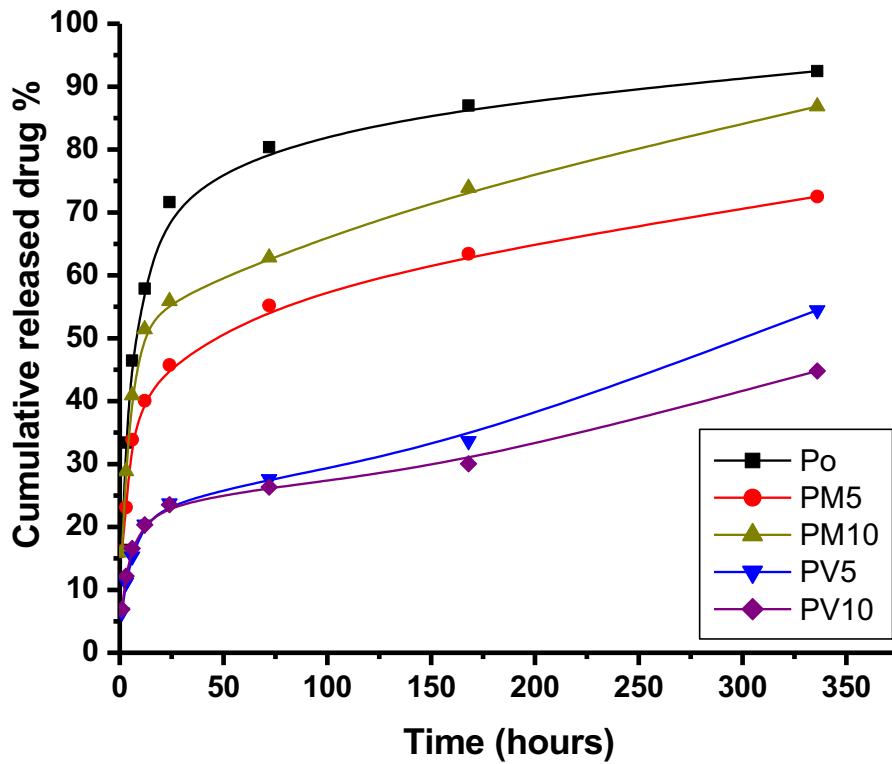


Figure 8. SEM photographs and EDX analysis of the different phosphate glasses after immersion in SBF for 7 days



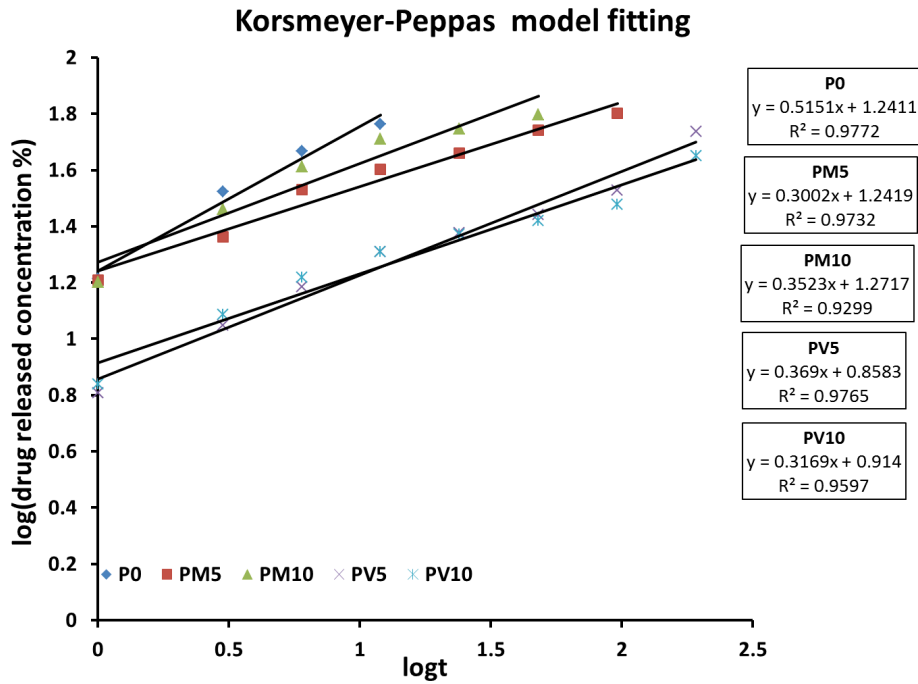


Figure 9. Vancomycin drug release profiles of the different phosphate glasses (P0, PM5, PM10, PV5 and PV10) using tris-buffer (pH 7.4) as incubating medium, and Higuchi and Korsmeyer-Peppas models fitting.

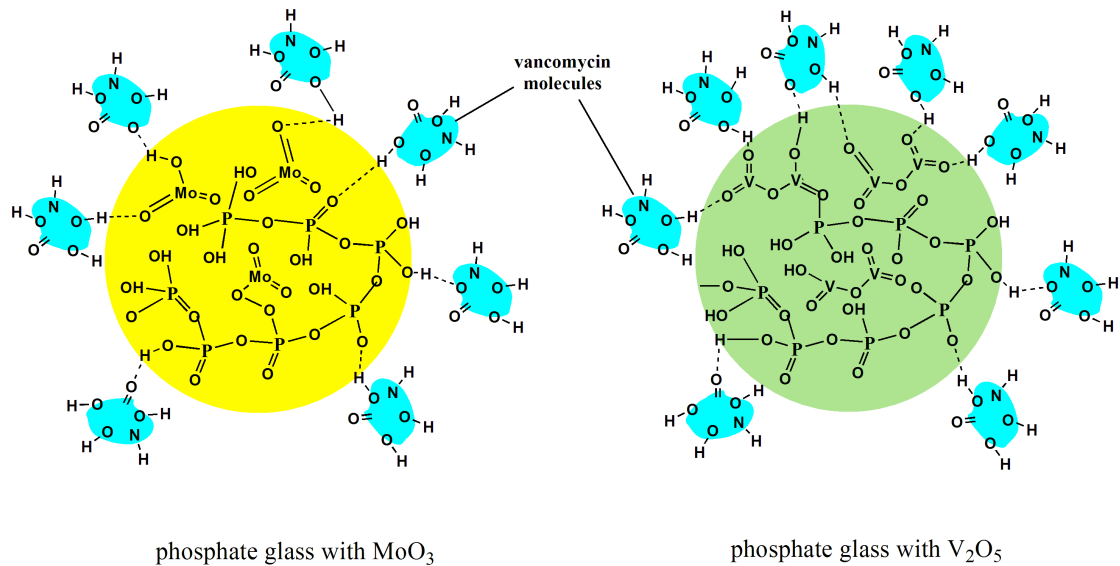


Figure 10. a schematic diagram of Vancomycin molecules bonded with Mo- and V-containing phosphate glasses surfaces by hydrogen bonding